JOURNAL OF MATERIALS SCIENCE **37** (2002) 4733–4741

Processes and states during polymer film formation by simultaneous crosslinking and solvent evaporation

M. DUŠKOVÁ-SMRČKOVÁ
Institute of Macromolecular Chemistry, Academy of Sciences of the Czech Republic, 162 06 Prague 6, Czech Republic; Faculty of Mathematics and Physics, Charles University, Prague, Czech Republic

K. DUŠEK*
Institute of Macromolecular Chemistry, Academy of Sciences of the Czech Republic, 162 06 Prague 6, Czech Republic
E-mail: dusek@imc.cas.cz

Coating film formation with simultaneous crosslinking and solvent evaporation, accompanied by passage of the polymer film through glass transition region, is a complex process by which temporary or permanent anisotropic and gradient network structures can be formed. Evaporation and crosslinking are processes that are interdependent. The changes in structure (growth of branched molecules and network evolution) are a function of reaction kinetics, which gets diffusion controlled when the system passes through the glass transition region. Structural changes are determined by branching, gelation, and network build-up and depend on the architecture of network precursors. Thermodynamic interactions of polymer with solvents affect the solvent activity which determines the vapor pressure of the solvent over the film and thus the evaporation rate. The glass transition temperature increases as a result of both the decreasing solvent content and conversion of functional groups into bonds. By interplay of these two factors more or less solvent can be locked in by vitrification. The roles and intensity of these basic processes and interrelations are discussed. Some older results are reviewed and new experimental evidence is added. The interrelations are illustrated by time dependences of solvent evaporation and conversion of functional groups for solvent-based high-solids polyurethane systems composed of a hydroxyfunctional star oligomer and triisocyanate and by the role of the ratio of evaporation to crosslinking rates. Evidence was obtained of gradient formation in which appearance of a glassy surface layer is an important event in the history of film formation that determines solvent retention and other film characteristics.

1. Introduction

Simultaneous chemical crosslinking and solvent evaporation are the main processes that govern formation and quality of a majority of protective organic coating films. Solvent-based systems are directly concerned but understanding of the role of these processes is important also for water-born dispersions where certain amounts of auxiliary solvents are used.

These two basic processes are characterized by amount of solvent evaporated (weight loss) and increase of conversion of reactive groups. Both are interdependent and are functions of (drying) time. Formation of chemical bonds and decrease of solvent content are controlled by diffusion of solvent molecules out of the film and induce changes in structure and static and dynamic properties of the polymer-solvent system.

- Chemical reaction proceeds by which molecular weights of the polymer binder increase, the system passes through the gel point, and a three-dimensional network is building-up.
- The segmental mobility decreases (glass transition temperature, T_g, of the system increases) as a result of both the progress of crosslinking reaction and decrease in solvent concentration.
- Stresses are developing as a result of shrinkage caused both by solvent evaporation and contraction due to formation of covalent bonds.

*Author to whom all correspondence should be addressed.

- Gradients of solvent concentration, conversion of functional groups, and structure are developing due to transport of solvent from the film interior to the surface.

The case when the system during drying passes through the main transition region, i.e., from melt/rubber to glass is quite frequent (ambient temperature crosslinking) and rather complex. When T_g approaches or exceeds the reaction temperature, the curing reaction becomes diffusion-controlled and greatly retarded; also the diffusion rate of solvent molecules decreases considerably and, as a result, the solvent evaporation slows down. The interdependence of rates of basic processes, conversion of functional groups into bonds and decrease in solvent concentration, is highlighted by the following correlations:
The *reaction rate* depends on solvent amount and quality through

- groups concentration;
- segmental mobility (T_g);
- groups microenvironment (local polarity, fluctuations in group concentrations);
- possible faster migration of one of the components in the early stages of reaction resulting in local off-stoichiometry;
- possible phase separation assisted by solvent presence.

The *evaporation rate* depends on solvent volatility, rate of transport of solvent molecules through the film, on partial pressure of solvent vapor at the film surface, which is proportional to solvent volatility and its activity in the film. The solvent transport is driven by the thermodynamic gradient. These quantities depend on conversion of functional groups through

- molecular weight/crosslinking density of polymer;
- diffusivity of solvent molecules determined by their size and shape, interaction with the polymer and segmental mobility of the polymer (T_g);
- stresses developed by shrinkage due to bond formation and solvent evaporation;
- phase separation assisted by increase in molecular weights/crosslinking density.

Most of the basic features of film formation and the above discussed interdependences have been qualitatively understood (cf., e.g., [1–3] and the gradient character of the drying film proved and quantified using various in-depth profiling techniques such as ATR (attenuated total reflection) FTIR and Raman spectroscopies, photoacoustic FTIR and one-dimensional magnetic resonance imaging (cf., e.g., [4–12]). Also stresses are developed during drying of the films. The stresses are characterized by bending of a thin steel foil substrate [13–15]. Diffusion processes controlling drying of films were analyzed by Vrentas and Vrentas [16] and Paul [17].

The so-called *solvent retention* or *solvent entrapment* (retention of some residual solvent in the coating film even after long drying times) and permanent stresses generated by network deformation in adhering films [18] are very serious problems affecting the quality and durability of coating films [19–20].

Very important in optimization of composition and the conditions of the film forming process is not only the choice of the type of crosslinking reaction, chemical nature of the binder and quality of the solvent, but also the structure (architecture) of the binder–precursor of the polymer network [21–23]. Even with precursors of the same molecular weight and equivalent weight per group, network formation—evolution of molecular weights, gel point, sol-gel transition and build-up of crosslinking density (concentration of elastically active network chains)—can greatly differ (cf., e.g., a telechelic polymer *vs.* star *vs.* hyperbranched polymer). Because of the difference in network structure, also the polymer-solvent interaction is different and, consequently, so is the solvent activity and rate of evaporation. The rate of evaporation strongly depends on convection in the vapor phase. Under static conditions, the evaporation rate, especially in the earlier stages of film formation, is determined by diffusion through the gas layer above the film, whereas at later stages the diffusion through glass becomes so slow that it dominates the evaporation rate.

In this contribution, we discuss very briefly physical and chemical factors of processes controlling film formation by simultaneous crosslinking and solvent evaporation: solvent vapor pressure determined by thermodynamics of polymer-solvent system, kinetics of the crosslinking reaction and network build-up in dependence on network precursor architecture. Results already published are reviewed and analyzed from the standpoint of new theoretical development. In the second part, some examples are shown of formation of a coating film from two-component polyurethane solvent-based high-solid formulations, where diffusion control by segmental mobility sets in.

2. Basic parameters determining solvent vapor pressure over films

2.1. Thermodynamic factors

The vapor pressure of solvent, p_1, in equilibrium with a polymer-solvent mixture is determined by the activity of the solvent, a_1,

$$p_1 = p_1^0 a_1 = \exp(\Delta\mu_1/\mathrm{R}T) \tag{1}$$

where p_1^0 is the vapor pressure of the pure solvent at temperature T and $\Delta\mu_1$ is the change of chemical potential of the solvent associated with mixing of solvent with polymer segments. In the classical model [24–26] of polymer network–solvent systems, the additivity of contributions to Gibbs energy by mixing and network deformation is assumed

$$\Delta G_{\mathrm{swell}} = \Delta G_{\mathrm{mix}} + \Delta G_{\mathrm{net}} \tag{2}$$

For Gaussian chains

$$\frac{\Delta G_{\mathrm{net}}}{\mathrm{k}T} = An_{\mathrm{e}}\left(\Lambda_x^2 + \Lambda_y^2 + \Lambda_z^2 - 3\right) - Bn_{\mathrm{e}}\ln(\Lambda_x\Lambda_y\Lambda_z) \tag{3}$$

where Λ_k is the deformation ratio in the direction of the k axis with respect to isotropic reference state at which the chains have their unperturbed dimensions; n_e is the number of elastically active network chains. The factors A and B are discussed below. Equations 2 and 3 determine vapor-gel and liquid-gel (swelling) equilibria under unstrained or strained conditions.

For isotropic swelling in solvent vapor or liquid, $\Lambda_x = \Lambda_y = \Lambda_z = \Lambda$, and the deformation ratio Λ is related to the volume fraction of the polymer ϕ_2 as

$$\Lambda = \phi_2^{-1/3}\left(\phi_2^0\right)^{1/3} \tag{4}$$

where ϕ_2^0 refers to the reference state at network formation; ϕ_2^0 is assumed to be equal to the volume fraction of polymer during network formation. Adding the Flory-Huggins mixing term and differentiating ΔG_{swell}, chemical potentials are obtained. The equilibrium degree of swelling in solvent or its vapor is determined by the equality of chemical potentials of solvents, μ_1, in both phases.

$$\frac{\Delta\mu_1}{RT} = \ln a_1 = \ln(1-\phi_2) + \phi_2\left(1 - \frac{1}{x}\right) + \chi\phi_2^2 + \nu_e\bar{V}_1\left(A\left(\phi_2^0\right)^{2/3}\phi_2^{1/3} - B\phi_2\right) \tag{5}$$

In this equation, χ is the polymer-solvent interaction parameter, x is the ratio of molar volumes of the polymer (number average) and solvent, ν_e is the concentration of elastically active network chains in a volume unit, $\bar{V}_1$ is the molar volume of the solvent. A and B are factors in the rubber elasticity theory ($A = 1$, $B = 2/f$ (f is effective functionality of the crosslink) for the affine model, and $A = (f-2)/f$ and $B = 0$ for the phantom network model [24, 25]). (In [18], the equations are valid for networks with tetrafunctional crosslinks, $2/f = 1/2$ and the value of B used there for the affine was equal to 1).

Equation 5 can be used for uncrosslinked solutions and swollen networks as well. Below the gel point, at which infinite structure appears in the system for the first time, $\nu_e = 0$ and x increases. Beyond the gel point, in equilibrium with an excess of liquid solvent, sol is extracted and $1/x = 0$; ν_e can be determined as a function of conversion of the crosslinking reaction. If sol is not extracted (swelling in solvent vapor), the situation is more complex and approximations must be used.

A similar approach was used for an anisotropic network adhering to the substrate and strained in plane by evaporating solvent. During solvent evaporation, only the thickness changes (the coordinate x by definition), and the y and z dimensions do not change. The relations between extension ratios are as follows

$$\Lambda_x = L_x/L_{0x}, \quad \Lambda_y = \Lambda_z = 1$$

(L is length) and

$$\Lambda_x = \frac{L_x}{(L_x)_{dry}}\frac{(L_x)_{dry}}{L_{0x}} = \phi_2^{-1}\phi_2^0 \tag{6}$$

Then [18]

$$\frac{\Delta\mu_1}{RT} = \ln(1-\phi_2) + \phi_2(1-1/x) + \chi\phi_2^2 + \nu_e\bar{V}_1\left[A\left(\overline{\phi_2^0}\right)^2\phi_2^{-1} - B\phi_2\right] \tag{7}$$

The factor $\overline{\phi_2^0}$ characterizes the state of network chains in the dry state relative to the (relaxed) state at network formation. For fast crosslinking relative to evaporation, $\overline{\phi_2^0}$ is equal to the initial volume fraction of the polymer in the coating. For simultaneously occurring solvent evaporation and crosslinking it is a mean value over the range of concentration of elastically active network chains starting from the gel point at which $\nu_e = 0$

$$\overline{\phi_2^0} = \frac{1}{\nu_e}\int_{\nu=0}^{\nu_e}\left(\phi_2^0\right)d\nu \tag{8}$$

where the instantaneous dilution factor is equal to the instantaneous volume fraction of the polymer $\phi_2^0(\nu_e) = \phi_2(\nu_e)$. Very slow crosslinking relative to solvent evaporation means that crosslinking takes place practically in the dry state (if the system is still above T_g) and very little strain is developed (only due to reaction contraction).

An important result follows from Equation 7 [18] that strains in plane developed as a result of solvent evaporation (equivalent to biaxial extension) lower the solvent activity, i.e., they assist retention of solvent in the film.

Equation 7 also describes changes of vapor pressure produced by the crosslinking reaction at constant content of solvent ϕ_2. Continuing bond formation changes x, χ, ν_e and could have an effect on A and B

- *before the gel point*, $\nu_e = 0$, x increases (it is proportional to the degree of polymerization or molecular weight of the polymer), and χ changes; whether it increases or decreases with increasing conversion depends on the particular crosslinking system. The increase in x causes an increase in $\Delta\mu_1$ and solvent activity a_1. The change in x can be calculated by the branching theory as a function of conversion and the change in χ by one of the contribution methods (e.g., from solubility parameters)
- *beyond the gel point*, ν_e increases and the elasticity term comes into play and the solvent activity also depends on the state of network chains relative to the state of normal coiling given by $\overline{\phi_2^0}$; χ continues changing. Sol is still present but usually its fraction decreases steeply. Its molecular weight also decreases. At a certain distance from the gel point, the effect of the presence of a small fraction of sol on $\ln a_1$ can be neglected. However, in the intermediate range it may play a role and should be considered, e.g., by adding sol and gel contributions (similar to *single-liquid approximation* for binary solvent–polymer systems [27]). Alternatively, the system can be treated as a quasiternary one, taking

the polydisperse sol as one component and the network as another one. The dependences of w_s and ν_e on conversion of functional groups are provided by branching theories.

At a fixed ϕ_2, the solvent activity a_1 usually increases as a result of crosslinking and its value may reach 1. When this happens, the system phase separates either in the form of microsyneresis (development of turbidity) or macrosyneresis (separation of a bulk liquid phase) [23, 28, 29]. Both forms of phase separation were observed during formation of polyurethane films. In drying films, where crosslinking is accompanied by solvent evaporation, the increase in a_1 due to bond formation is compensated by increasing ϕ_2, so that phase separation usually does not take place. However, a danger of phase separation always exists for "slow" solvents. It is useful to balance the system in such a way that the solvent activity is kept close below 1, so that in the course of drying the evaporation rate does not decrease much.

Equation 3 is a first approximation to the real case especially as far as phase equilibria is concerned because a polydisperse system is approximated by a single component. Also, the non-glassy state of the system is assumed. In glassy systems, phase separation is no longer possible. The predicted correlation of p_1 with network composition was confirmed by direct measurement of vapor pressure [30] but no information is available about solvent vapor pressure over polymer-solvent glasses.

2.2. Crosslinking kinetics

All parameters affecting vapor pressure of the solvent have been expressed in the preceding section as a function of conversion. Since diffusion and evaporation are expressed as a function of time, it is necessary to express conversion as a function of time. With exception of free-radical chain reactions, there is not much difference in kinetics of linear and crosslinking polymerization reactions. Increasing polydispersity and passage through the gel point usually have a subtle effect on reaction rate [31]. A very crucial event in film formation history is the onset of reaction rate control by segmental diffusion when the system passes through the main transition zone. The apparent rate constant, which is a constant in the region of control by chemical reactivity, starts falling down sharply [32]. This is because the rate constant for reaction between groups A and B controlled by segmental mobility, $k_{AB,D}$ gets smaller than that determined by chemical reactivity, $k_{AB,C}$. According to the Rabinowitch equation, the apparent rate constant is a function of both as

$$\frac{1}{k_{AB,app}} = \frac{1}{k_{AB,D}} + \frac{1}{k_{AB,C}} \tag{9}$$

The quantity $k_{AB,D}$ is proportional to the diffusion coefficient of segments D_{segm}, $k_{AB,D} \propto D_{segm}$ and D_{segm} is a function of free volume as

$$D = D_0 \exp\left(\frac{b_D}{f_g + \alpha_f(T - T_g)}\right) \tag{10}$$

In this expression b_D is a constant, f_g is the fractional free volume at temperature T_g, and α_f is the thermal expansion coefficient of free volume. Since T_g depends on conversion (several relations are discussed in [33]), $k_{AB,app}$, the "constant" we determine from experiment, also depends on conversion. It has been confirmed by several studies that the dependence of T_g on conversion, α, is independent of reaction temperature. Typically, $k_{AB,app}$ is independent of conversion of functional groups until a region close to T_g is reached, and then starts falling sharply as the denominator in Equation 10 approaches zero [32].

The presence of solvent is another factor influencing T_g. It falls down with increasing volume fraction of solvent, ϕ_1, (decreasing ϕ_2) as [34]

$$T_g(\phi_1, \alpha) = \frac{\phi_1 T_{g1} + \phi_2[(1-\alpha)K_1 T_{g0} + \alpha K_2 T_{g\infty}]}{\phi_1 + \phi_2(1-\alpha)K_1 + \alpha K_2} \tag{11}$$

where K_1 and K_2 are constants characteristic of the given polymer-solvent system, T_{g1}, T_{g0}, and $T_{g\infty}$ are T_g values for the solvent, uncrosslinked system, and fully crosslinked system, respectively.

2.3. Solvent diffusivities

Diffusion of solvent is driven by the thermodynamic gradient. In the non-glassy systems, the solvent diffusion during evaporation from a polymer film was analyzed in detail (cf., e.g., [16, 17]). When glass transition interferes, diffusion is more complex (e.g., dual state of solvent molecules in the glass—Henry and Langmuir type, and aging of polymer glasses with rates comparable with film formation rates [35]).

2.4. Evaporation mode

Diffusion of solvent through the polymer film with a gradient in the film or the gradient in the gas layer adjacent to the film surface can be evaporation rate controlling processes. Under practical conditions of ambient temperature film formation, the mechanism of evaporation is obviously mixed. Later stages of diffusion are controlled by gradient in the polymer film. In that case, the rational way to model film formation is the use of finite element method as demonstrated by [2, 3] and [36].

The control by the gradient of solvent vapor concentration in the gas film over the coating is not fully unrealistic for slowly evaporating solvents in the absence of convection of the gas phase. In that case, the amount of solvent penetrating through unit square area per time unit q is equal to

$$\frac{dq}{dt} = \frac{D}{l'} c_1 \tag{12}$$

where D is the coefficient of diffusivity of solvent through the gas phase, l' is the gas film thickness and c_1 is the concentration of solvent in the gas phase adhering to the coating film surface (it is assumed that at

the distance l' the solvent concentration drops to zero). The concentration of solvent molecules in vapor at the film surface, c_1, is proportional to partial pressure of solvent which is proportional to solvent activity a_1

$$p_1 = p_1^0 a_1 \tag{13}$$

For high solid rubbery systems of not too high crosslinking density, one finds from Equation 5

$$a_1 \approx \phi_1 \tag{14}$$

Using mass balance condition, the solution of Equation 12 is

$$\phi_1 = \phi_1^0 \exp\left(- \frac{Dc_1^0}{ll'} t \right) \tag{15}$$

where ϕ_1^0 is the initial volume fraction of the solvent in the film, l is the coating film thickness and

$$c_1^0 = p_1^0 M_1 / \mathrm{R}T \tag{16}$$

where M_1 is the molecular weight of the solvent.

Combination of diffusion equation (15) with vapor pressure equations (5) or (7), kinetic equation (9) segmental mobility equations (10) and (11), and branching theory offering changes in structural parameters, can be used for predicting crosslinking and evaporation rates as well as changes in the glass transition temperature T_g. Fig. 1 shows a model example of changes of the reaction rate and T_g as a function of time for a diepoxide-diamine system [32]. The acceleration of the reaction is caused by an increase in the reactant concentration due to solvent evaporation. The subsequent decrease of reaction rate is caused by decreasing segmental mobility when glass transition sets in.

2.5. Network build-up

The increase in molecular weights, position of the gel point, increase in the gel fraction, w_g, and concentration of elastically active network chains, ν_e, are important input parameters determining the activity of solvent in the film. For a majority of crosslinking systems used in coatings, the statistical theory of branching processes is applicable and very convenient. The basics [23, 37] and application to crosslinking of polyurethanes [38], epoxide resins [39], crosslinking of primary chains [40] and unsaturated systems [41] have been described elsewhere. The structures—molecules before the gel point in the sol and various substructures in the gel (dangling chains, elastically active chains and elastically active crosslinks) are generated from building units in different reaction states. The building units are identical with component units or their fragments. The reaction states differ in the number of reacted functional groups and types of bonds extending from them. The distribution of building units in different reaction states is described by probability generating function $F_0(\mathbf{z})$ which bears all information about the states of the system. All structural parameters listed above are obtained by standard operations without any additional information. We will highlight some of the recent applications of the theory to crosslinking systems used for coatings:

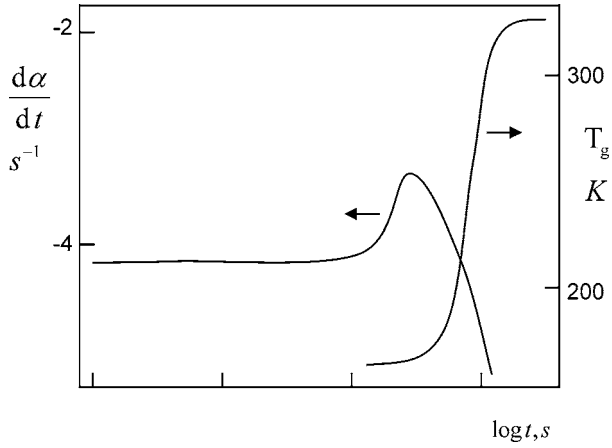

Figure 1 Simulated dependence of reaction rate $d\alpha/dt$ (α is conversion of functional groups) and increase of the glass transition temperature T_g; slowly evaporating solvent; diepoxide-diamine system of [32] with 50% solvent.

2.5.1. Functional stars

Crosslinking of hydroxy-functional stars of different functionality and groups of different reactivity were studied [42–44]. The crosslinker was a trifunctional isocyanate. Bond formation was based on reaction of an isocyanate group (—NCO) with a hydroxy group (—OH) giving a urethane bond (—NH.CO.O—) [45]. It was predicted theoretically and confirmed experimentally, that a monodisperse star gels at higher conversion and longer reaction time than a blend of stars of different functionality that has the same average functionality as the monodisperse star. Likewise, a tetrafunctional star having, for instance, two OH groups of higher and two OH groups of lower reactivity gels later than a 1:1 blend of two stars having each all four groups of higher or lower reactivities (cf. Fig. 2). This is due to the fact that gelation is determined by second moments of functionality and reactivity distributions.

2.5.2. Telechelic polymers and copolymers

Classical telechelic polymers have two functional groups at their extremities. Their polydispersity can be low depending on the polymerization or copolymerization technique used. Polyfunctional crosslinkers have to be used. Cyclization is usually weak and theoretical treatment of network formation relatively easy [38, 46]. High conversions of functional groups can be reached and the network can be relatively defectless. Due to their low functionality, the concentration of EANCs is low and they are more frequently used in preparation of crosslinked elastomers.

2.5.3. Functional copolymers

Low-molecular-weight copolymers of a functional monomer with one or several modifying non-functional

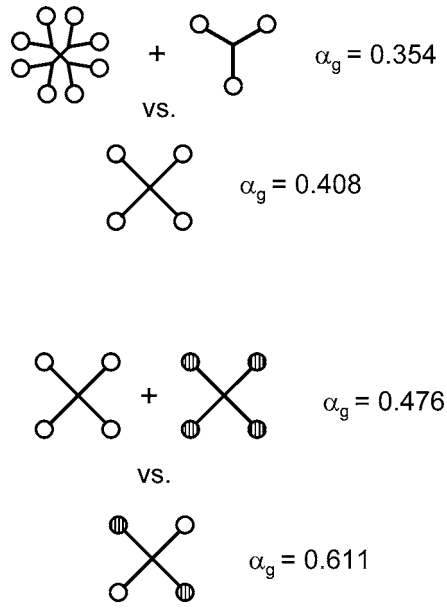

Figure 2 Comparison of crosslinking of single component hydroxy-functional stars and blends of functional stars; crosslinker: trifunctional isocyanate. Upper part: blend of octa- and trifunctional stars vs. a tetrafunctional star; lower part: blend of two tetrafunctional stars with groups of different reactivity vs. star with two groups of higher and two groups of lower reactivity; reactivity ratio of primary to secondary OH groups equal to 10; NCO group conversions at the gel point α_g indicated.

monomers are quite common and inexpensive precursors. In hydroxy-functional precursors hydroxyethyl-, or 2-hydroxypropyl methacrylates or acrylates are used as functional monomers and the modifying comonomers are selected so as to adjust thermal or aging properties or compatibility with the solvent and crosslinker. Distributions are characteristic of these precursors: distribution in degree of polymerization, distribution in molecular weight, distribution in the number of functional groups, and sequence distribution making the sequences of functional groups more or less blocky (Fig. 3).

Existence of these distributions has a large effect on network formation and structure. A statistical functional copolymer contains fractions of copolymers

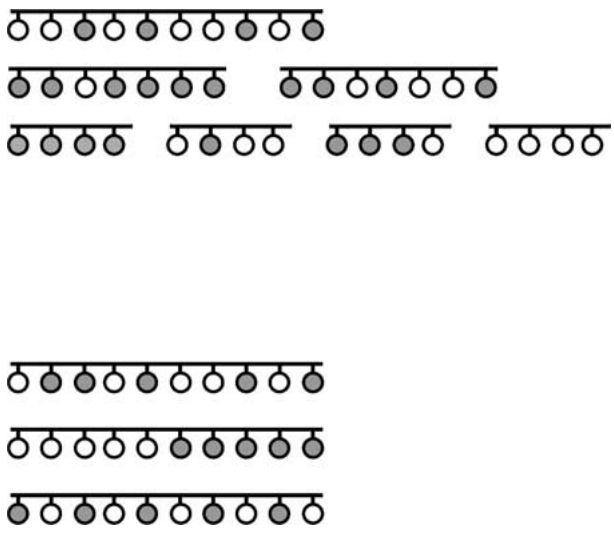

Figure 3 Sketch showing degree-of-polymerization, compositional distribution, and sequence distribution of copolymers (grey circle is a functional (crosslinking) group, white circle a non-functional group).

with no or one functional group as well as copolymers with many functional groups. This gives rise to the existence of a sol fraction even in stoichiometric systems at 100% conversion of functional groups. The gel point is shifted to lower conversion (control by the second moment of functionality distribution). Existence of branch points in the functional copolymer chain is another special feature of this system. During crosslinking, these branch points get active and they gradually contribute to the increase in concentration of elastically active network chains (EANC). The theory of branching processes is very well suited for handling various distributions. Thus, the degree of polymerization and compositional distributions are incorporated into the basic generating function $F_0(\mathbf{z})$ again in the form of generating functions. In Fig. 4, crosslinking of statistical functional copolymers and telechelic polymers with trifunctional crosslinker is compared. The same average functionality as of the telechelic copolymer, i.e., $f = 2$, and the same molecular weight was selected for the statistical copolymer. The results of calculations [47] show that the gel fractions and concentrations of EANCs are quite different. The statistical copolymer gels earlier and the sol fraction is present even at 100% conversion because of functionality and degree-of-polymerization distributions. The concentration of EANCs is higher for the statistical copolymer because of the contribution made by internal branch points; the telechelic polymer cannot contribute by any branch point.

The contemporary polymerization techniques make it possible to vary the sequence distributions in copolymers. Functional copolymers with units carrying functional groups arranged in blocks, distributed statistically or alternating are typical examples (Fig. 3). The differences in sequence distribution may have an important effect on network formation and structure for two reasons: there can exist an effect of (a) the nature of the neighbor monomer unit on the reactivity of the functional group (neighbor effect), and (b) local environment on concentrations of reactive groups (concentration fluctuations) and local polarity, dielectric

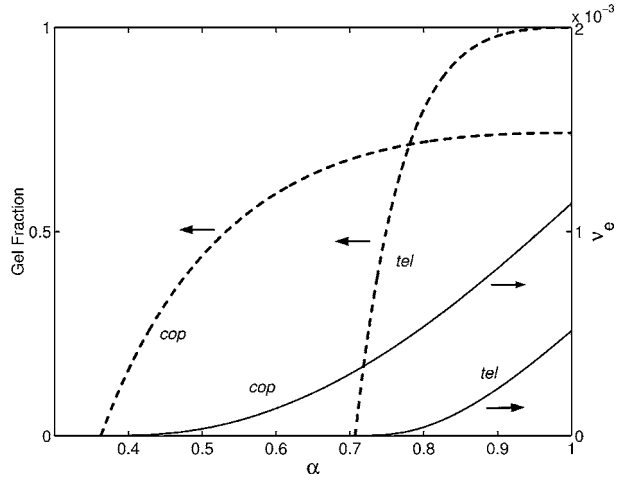

Figure 4 Comparison of evolution of gel fraction and concentration of elastically active network chains, ν_e, for crosslinking of a telechelic polymer (tel) and a statistical copolymer (cop) with most probable distribution of degrees of polymerization and of number-average functionality $f_n = 2$. Number-average molecular weights, $M_n = 2000$. Trifunctional crosslinker, $M = 500$; stoichiometric ratio of NCO : OH groups.

constant(microenvironment effect). Such effects can be positive or negative. In the case of positive effect, the groups of longer sequences of the functional monomer units react faster. This leads to an alteration of distribution of the number of reacted functional groups per copolymer molecule. The molecules richer in longer sequences of functional monomer units are even richer in the number of bonds extending to the crosslinker. Therefore, the gel point is shifted to lower conversions and structural characteristics (w_g or ν_e) are altered. Both the neighbor effect and microenvironment effect were found to be operative in crosslinking of glycidyl methacrylate copolymers with diamines. Block copolymers gel faster and at lower conversions than the statistical ones of the same number of functional groups per chain, both having the same and narrow molecular weight distribution. The existence of the neighbor effect was proved by model reaction of the copolymer with secondary amine in good solvent [21, 48]. The evidence of the microenvironment effect was observed for the crosslinking when solvent quality was varied.

2.5.4. Functional hyperbranched polymers

Hyperbranched polymers prepared from BA_f monomer and carrying functional groups A are precursors for coatings which are not explored sufficiently as yet. Unlike functional dendrimers, their degree of polymerization distribution is an important factor. Ideally, the polydispersity of hyperbrached polymers diverges at full conversion of minority groups, but there exist ways to make the distribution somewhat narrower. Two major problems in application of hyperbranched polymers as binders are encountered: (a) the solubility is usually poor due to many (polar) functional groups and (b) the functionality is too high, so that gelation occurs early. Both problems can be resolved by modification of endgroups resulting in improvement of solubility and processability. The advantage of hyperbranched monomers for application in coatings is still to be assessed. From the point of view of theoretical modeling, hyperbranched polymers (HBP) are an example where the same theoretical method can be used for generation of the precursor distribution and for its crosslinking. The information obtained by simulation of HBP distribution in the form of generating function is an input information for crosslinking [49]. Such an approach was used before for simulation of a multistage crosslinking process associated synthesis and crosslinking of powder coatings [50, 51].

There are many other instances of application of branching theories in the thermoset and elastomer field, e.g., for curing of epoxy resins.

3. Main characteristics of coating film formation

In this section, the main features of film formation from high-solid formulations of a hydroxy-functional star and triisocyanate obtained by cyclotrimerization of hexamethylene diisocyanate (HDI trimer) are summarized. The star was a tetrafunctional oligomer of the type described in [42–44] of equivalent weight ~250 g/eq. The weight loss due to solvent evaporation was monitored by a recording balance and the progress of crosslinking reaction by a decrease in concentration of NCO groups using transmission and ATR FTIR, where by ATR changes in only 1–2 μm surface layer are seen. T_g was determined by dynamic mechanical analysis. Various solvents and solvent concentrations were studied. Also the effect of humidity in the air was investigated.

The strategy was such that, in parallel with open, evaporating films, network formation was studied in films closed between two glass or Teflon plates, where the concentration of solvent remained constant and no gradient of composition and properties developed. The crosslinking density (concentration of elastically active network chains, ν_e (cf., Equation 5) of these films was determined by equilibrium stress-strain measurements of swollen films and calculated from the shear modulus G_{sw}

$$\nu_e = \frac{G_{sw}}{RTA\left(\phi_2^0\right)^{2/3}\phi_2^{1/3}} \tag{17}$$

Here,

$$G_{sw} = f/(\lambda - \lambda^{-2})$$

f is tensile stress, and λ extension ratio.

The polymer-solvent interactions were characterized by the Flory-Huggins interaction parameter χ using the values of ν_e determined from G_{sw} by swelling equation (cf., Equation 5)

$$\chi = \frac{\ln(1-\phi_2) + \phi_2 + \nu_e \bar{V}_1\left(A\left(\phi_2^0\right)^{2/3}\phi_2^{1/3} - B\phi_2\right)}{\phi_2^2} \tag{18}$$

The crosslinking process was also characterized by determination of gel time at which the insoluble fraction appeared for the first time (extrapolation of the gel fraction to zero), and by conversion of functional (NCO) groups and by evolution of the gel fraction.

Fig. 5 shows the weight loss due to solvent evaporation as a function of time for different initial weight

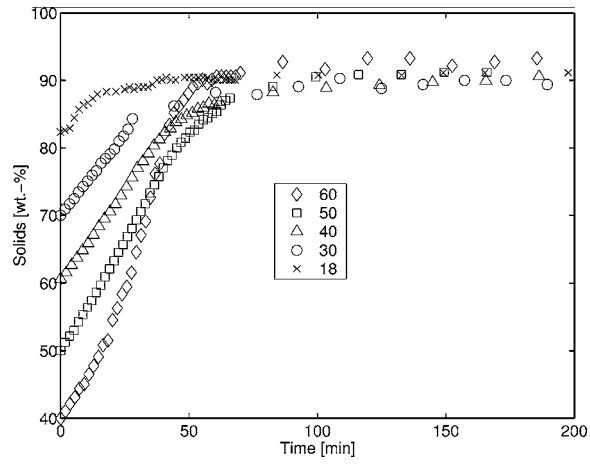

Figure 5 Weight loss due to solvent evaporation from crosslinking films (hydroxyfunctional star $f = 4$ and triisocyanate, stoichiometric ratio) of different initial solvent concentrations (in wt%) indicated; *Solids* represents weight fraction of non-volatiles; Solvent: methyl amyl ketone (MAK), 500 p.p.m. catalyst, wet thickness 200 μm; 25°C.

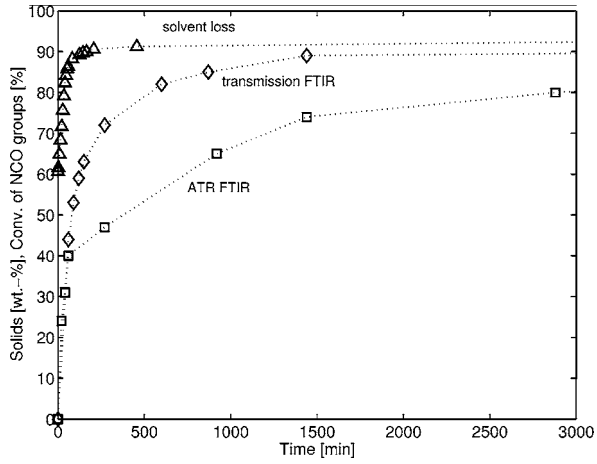

Figure 6 Weight loss due to solvent evaporation and conversion of NCO groups by FTIR in the whole film (transmission FTIR) and in the surface layer (ATR FTIR); initial solvent concentration 40 wt%, wet thickness 40 μm; other parameters as in Fig. 5

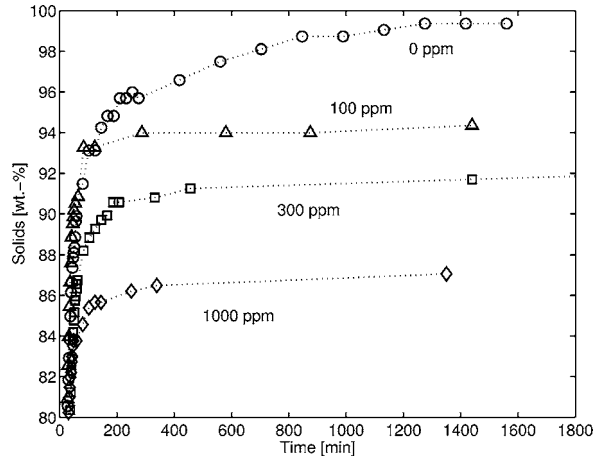

Figure 7 Weight loss due to solvent evaporation in dependence on catalyst concentration, the catalyst concentration indicated; wet thickness 200 μm; other parameters as in Fig. 5.

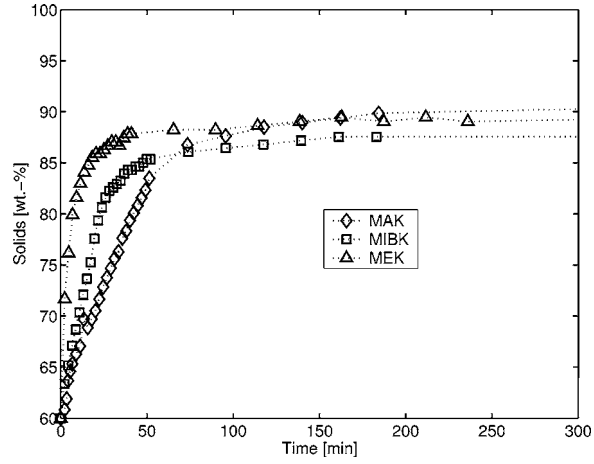

Figure 8 Weight loss due to solvent evaporation for three different ketones as solvents—methyl amyl ketone (MAK), methyl isobutyl ketone (MIBK), and methyl ethyl ketone (MEK), wet thickness 200 μm; other parameters as in Fig. 5.

fractions of solids. The initial rate is proportional to the solvent content but at a certain concentration level, the evaporation rate sharply drops and further evaporation is very slow—about 10% solvent remains entrapped in the film. Similar slowing down has been observed for the dependence of conversion of NCO groups on time (Fig. 6). When the conversion is measured by FTIR in the transmission mode, retardation of the reaction starts later and is less sharp in comparison with the solvent loss rate. At these times (gel point conversion ~35–40 mol%), the system has already passed through the gel point, i.e., from liquid to rubbery state. The ATR mode detects only changes in the surface layer 1–2 μm thick. Roughly from the onset of retardation of evaporation, the conversion of NCO groups to urethane bonds in the surface layer starts deviating from the conversion in bulk; the conversion in the surface layer is lower than in bulk. These results can be interpreted as due to formation of a glassy layer at the film surface due to a lower solvent concentration at the surface than in the bulk. The time when the rubber-glass transition starts at the surface roughly coincides with the drying time denoted as "dust-free time", whereas the pendulum hardness values are still low, feeling the rubbery interior of the coating layer.

The effect of the competition of the crosslinking rate and evaporation rate is seen in Fig. 7 showing the effect of organotin catalyst on evaporation rate. It is clearly seen that the solvent retention is the highest for the highest crosslinking rate. For the fastest reaction, the glass transition at the surface starts early due to fast structure build-up, and the least fraction of solvent could evaporate from the whole film because it cannot pass easily through the glassy layer. Therefore, the largest amount of solvent is locked in by the "skin". Without catalyst, the crosslinking rate is very slow and almost all solvent managed to evaporate before the conversion is high enough for the system to vitrify.

Compared to elastomers, these crosslinked polyurethane coatings have a relatively high crosslink density—the concentration of EANCs is of the order of 1000–2000 mol/m^3. The conventional solvents (ketones, esters) are relatively poor solvents (the parameter $\chi > 0.7$), ketones being generally better solvents than esters. The evaporation rate is primarily dependent on vapor pressures (boiling points) of pure solvent but at low solvent contents in the film the polymer-solvent interaction becomes important. Fig. 8 shows that the least volatile solvent, methyl amyl ketone, is retained least. This is so because fast evaporation of the more volatile solvent creates a steeper gradient and the glassy "skin" locks in more solvent than in the case of slow solvent. Also, a worse solvent (for methyl amyl ketone χ is the highest) has higher activity a_1 than a better one which is compensation for its lower volatility. The polymer-solvent interaction also affects to some extent the rate of crosslinking (the rate in poorer solvent is somewhat higher probably due to concentration fluctuations).

Because of a relatively high value of the interaction parameter and higher values of ν_e, the closed systems and evaporating systems containing a slow solvent are at the verge of their thermodynamic instability. Separation of bulk liquid phase was sometimes observed well beyond the gel point which is in line with the mode expected [23–29].

4. Conclusions

Coating film formation with simultaneous crosslinking and solvent evaporation, accompanied by passage of the film through glass transition region, is a complex process by which anisotropic and gradient network structures are formed. These processes are interdependent. They are determined by chemical and physical changes which can be described by thermodynamics and diffusion of macromolecular systems. The chemical reaction brings about changes in structure (growth of branched molecules and network evolution) which affect the thermodynamic interactions of polymer with the solvent, solvent activity and segmental mobility. The solvent activity determines the vapor pressure of the solvent over the film and evaporation rate. The content of solvent affects the rate of crosslinking reaction and passage from reactivity controlled to segmental diffusion controlled regimes. This contribution was aimed at stressing the role of these basic factors and ways of characterization of their roles and intensities. The effect of some of these factors was illustrated by study of film formation of polyurethane coatings.

References

1. S. VESSOT, J. ANDRIEU, P. LAURENT, J. GALY and J.-F. GÉRARD, *J. Coat. Technol.* **70**(822) (1998) 68.
2. R. A. CAIRNCROSS and L. F. FRANCIS, *Drying Technol. J.* **10** (1992) 893.
3. R. A. CAIRNCROSS, L. F. FRANCIS and L. E. SCRIVEN, *AIChE J.* **42** (1996) 55.
4. T. HIRAYAMA and M. W. URBAN, *Progr. Org. Coat.* **20** (1992) 81.
5. A. M. KAMINSKI and M. W. URBAN, *J. Coat. Technol.* **69**(872) (1997) 55.
6. *Idem.*, *ibid.* **69**(873)(1997) 113.
7. M. W. URBAN and C. L. ALLINSON, *ibid.* **71**(896) (1999) 73.
8. M. W. URBAN, C. L. ALLINSON, C. C. FINCH and B. A. TATRO, *ibid.* **71**(888) (1999) 75.
9. B.-J. NIU and M. W. URBAN, *J. Appl. Polym. Sci.* **70** (1998) 1321.
10. Q. HAN and M. W. URBAN, *ibid.* **81** (2001) 2045.
11. P. ZHANG, R. A. MISTRETTA and M. W. URBAN, *Polym. Mat. Sci. Eng.* **85** (2001) 105.
12. M. WALLIN, P. M. GLOVER, A.-C. HELLGREEN, J. L. KEDDIE and P. J. MCDONALD, *Macromolecules* **33** (2000) 8433.
13. E. M. CORCORAN, *J. Paint Technol.* **41**(538) (1969) 635.
14. A. A. STOLOV, T. XIE, J. PENELLE and H. L. HSU, *Macromolecules* **34** (2001) 2865.
15. J. A. PAYNE, L. F. FRANCIS and A. V. MCCORMICK, *Rev. Sci. Instrum.* **68** (1997) 4564.
16. J. S. VRENTAS and C. M. VRENTAS, *J. Polym. Sci. Polym. Phys. Ed.* **32** (1994) 187.
17. C. W. PAUL, *ibid.* **21** (1983) 425.
18. K. DUŠEK and M. DUŠKOVÁ-SMRČKOVÁ, *Polym. Bull.* **45** (2000) 83.
19. K. ADAMSONS, K. LLOYD and K. STIKA, in "Interfacial Aspects of Multicomponent Polymer Materials," edited by J. D. Lohse (Plenum Press, New York, 1997) p. 279.
20. K. ADAMSONS, G. BLACKMAN, B. GREGOROVICH, L. LIN and R. MATHESON, *Progr. Org. Coat.* **34** (1998) 64.
21. K. DUŠEK, *Trends Polym. Sci.* **5** (1997) 268.
22. K. DUŠEK, J. ŠOMVÁRSKY, M. SMRČKOVÁ, J. HUYBRECHTS and L. WILCZEK, *Polym. Mat. Sci. Eng.* **78** (1998) 223.
23. K. DUŠEK and M. DUŠKOVÁ-SMRČKOVÁ, *Progr. Polym. Sci.* **25** (2000) 1215.
24. P. J. FLORY, *Proc. R. Soc., Ser.* A **351** (1976) 351.
25. B. ERMAN and P. J. FLORY, *Macromolecules* **15** (1982) 806.
26. R. KONINGSVELD, W. H. STOCKMAYER and E. NIES, "Polymer Phase Diagrams. A Textbook" (Oxford University Press, 2001).
27. H. TOMPA, "Polymer Solutions" (Butterworth, London, 1956).
28. K. DUŠEK and J.-P. PASCAULT, in "Wiley Polymer Networks Group Review. Chemical and Physical Networks. Formation and Control of Properties," Vol. 1. edited by K. te Nijenhuis and W. Mijs (Wiley, 1998) p. 277.
29. K. DUŠEK, *J. Polym. Sci., Pt. C* **16** (1967) 1289.
30. G. ALLEN, P. EGERTON and D. J. WALSH, *Eur. Polym. J.* **15** (1979) 983.
31. K. DUŠEK, *Polym. Networks Gels* **4** (1996) 383.
32. K. DUŠEK and I. HAVLÍČEK, *Prog. Org. Coat.* **22** (1993) 145.
33. R. J. J. WILLIAMS, in "Polymer Networks. Principles of Their Formation, Structure and Properties" edited by R. F. T. Stepto (Blackie Academic and Professionals, 1998) p. 93.
34. G. ADAM and J. H. GIBBS, *J. Chem. Phys.* **43** (1965) 43.
35. W. R. VIETH, "Diffusion in and Through Polymers" (Hanser Publishers, Munich, 1991).
36. R. A. CAIRNCROSS, L. F. FRANCIS and L. E. SCRIVEN, *Drying Technol.* **10** (1992) 893.
37. K. DUŠEK, in "Processing of Polymers, Material Science and Technology," Vol. 18, edited by H. E. H. Meijer (Wiley-VCH, Weinheim, 1997) p. 401.
38. *Idem.*, in "Telechelic Polymers: Synthesis and Applications," edited by E. J. Goethals (CRC Press, Boca Raton, 1989) p. 289.
39. *Idem.*, *Adv. Polym. Sci.* **78** (1986) 1.
40. *Idem.*, in "Polymer Networks. Principles of Their Formation, Structure and Properties," edited by R. F. T. Stepto (Blackie Academic and Professionals, 1998) p. 64.
41. K. DUŠEK and J. ŠOMVÁRSKY, *Polym. Internat.* **44** (1997) 225.
42. J. HUYBRECHTS and K. DUŠEK, *Surf. Coat. Int.* **81** (1998) 117.
43. *Idem.*, *ibid.* **82** (1998) 234.
44. *Idem.*, *ibid.* **82** (1998) 172.
45. D. STOYE and W. FREITAG, "Resins for Coatings. Chemistry, Properties and Applications" (Hanser Publ., 1996).
46. M. ILAVSKÝ, J. ŠOMVÁRSKY, K. BOUCHAL and K. DUŠEK, *Polym. Gels Networks* **1** (1993) 159.
47. M. DUŠKOVÁ-SMRČKOVÁ, K. DUŠEK, X. JIANG, P. SCHOENMAKERS, V. LIMA, G. VAN BENTHEM-VAN DUREN and R. VAN DER LINDE, in Proc. Europolymer Congress, Eindhoven, 2002, Section , keynote lecture.
48. K. DUŠEK, *Polym. Mat. Sci. Eng.* **74** (1996) 170.
49. K. DUŠEK and M. DUŠKOVÁ-SMRČKOVÁ, in "Dendritic Polymers," edited by D. A. Tomalia and J. M. J. Fréchet (Wiley, 2002) p. 111.
50. G. P. J. M. TIEMERSMA-THONE, B. J. R. SCHOLTENS, K. DUŠEK and M. GORDON, *J. Polym. Sci. Polym. Phys.* **29** (1991) 463.
51. K. DUŠEK, B. J. R. SCHOLTENS and G. P. J. M. TIEMERSMA-THONE, *Polym. Bull.* **17** (1987) 239.

Received 15 April
and accepted 12 June 2002